Letter   Editors' Suggestion

Kinetics of formation of a macroscale binary Coulombic material

Sarah Battat ⬤,[1] Amit A. Nagarkar,[2] Frans Spaepen,[1] David A. Weitz,[1,3,4,*] and George M. Whitesides[2,†]

[1]*John A. Paulson School of Engineering and Applied Sciences, Harvard University, Cambridge, Massachusetts 02138, USA*
[2]*Department of Chemistry and Chemical Biology, Harvard University, Cambridge, Massachusetts 02138, USA*
[3]*Department of Physics, Harvard University, Cambridge, Massachusetts 02138, USA*
[4]*Wyss Institute for Biologically Inspired Engineering, Harvard University, Boston, Massachusetts 02115, USA*

The electrostatic self-assembly of charged Brownian objects typically occurs in cases of short-range interactions. The objects form Coulombic materials that are close-packed and have long-range order. Here, we present a system in which two kinds of non-Brownian millimeter-sized beads tribocharge differently, experience long-range electrostatic interactions, and still form ordered two-dimensional structures. We provide a complete characterization of the kinetics of formation of these materials, as the total number of beads is held constant and the relative number of beads that tribocharge negatively or positively is modified. We agitate the beads by shaking the dish in which they are contained. We show that the beads commonly adopt a transient structure that we call a *rosette*. A rosette consists of a central bead surrounded by six close-packed neighbors of a different kind. The symmetry of the final structure depends on the relative number of negatively and positively charged beads, and it is not necessarily the same as that of the transient structure. Our results bear important implications in the *de novo* design of Coulombic materials given our ability to isolate transient structures, identify the moment of their appearance, and quantify the impact of agitation, tribocharging, and Coulombic energy minimization on their persistence.

I. INTRODUCTION

Electrostatic self-assembly refers to the formation of a Coulombic material whose constituent elements interact electrostatically. Generally, charged objects that undergo Brownian motion interact at short range, meaning that their screening lengths are comparable with their size [1–4]. Since electrostatic interactions are short range, the objects tend to form close-packed ordered structures. In contrast, when interactions are sufficiently long range, such that screening lengths exceed the size of the objects, Brownian objects can flocculate irreversibly and form disordered aggregates [3]. In exceptional circumstances, however, it is possible to produce ordered structures from charged objects with long-range interactions [5,6]. Here, we present a similar system where nylon and polytetrafluoroethylene (PTFE) beads, each measuring approximately 2.38 mm in diameter, assemble into two-dimensional (2D) ordered structures, notwithstanding their long-range electrostatic interactions. These beads are non-Brownian, and their interaction energy scales as $1/r$, where r is the radial distance from their center [7]. They move inside a metal-coated, ungrounded Petri dish that is mechanically agitated, charge by tribocharging, and interact via Coulombic forces. The combined total number of nylon and PTFE beads is maintained constant, while the relative number of nylon and PTFE beads is altered. Authors of previous studies [5,6] have characterized some steady-state structures formed by

tribocharged beads; however, a description of the kinetics of their formation was lacking. To design Coulombic materials, knowledge of *how* the materials form is important. In this letter, we set out to understand the dynamics of formation of a 2D binary Coulombic material composed of nylon and PTFE beads. We exclude three-dimensional (3D) materials from this study because the full dynamics of their assembly cannot be visualized using the techniques that we have developed. We show that the electrostatically self-assembled materials undergo local bead rearrangements to form final ordered structures. Transient structures that we call *rosettes* are common, and the symmetry of the rosette structure is usually different from the symmetry of the final structure. The symmetry of the final structures can be square, hexagonal, or pentagonal depending on the relative number of nylon and PTFE beads.

We study the formation of Coulombic materials from 400 initially uncharged beads that sit within a gold-coated Petri dish. The beads are made from either nylon, which is dyed blue, or PTFE, whose color is white. The relative number of nylon beads, N_{nylon}, and PTFE beads, N_{PTFE}, is varied such that $N_{nylon}/N_{PTFE} = \{\frac{1}{4}, 1, 4\}$. The beads occupy about 30% of the surface of a gold-coated Petri dish, or $\phi = 0.3$, as depicted schematically in Fig. 1(a). The Petri dish sits on the platform of either a linear or an orbital shaker, and its motion is restricted to a small area of the platform by a hard plastic enclosure with irregularly shaped sides (Fig. S8 in the Supplemental Material [8]). When the shaker is turned on, the dish begins to slide on the platform and bump into the sides of the enclosure. The beads move inside the dish and collide with the walls of the dish as well as with other beads; as a result of this motion and contact, the beads

*weitz@seas.harvard.edu
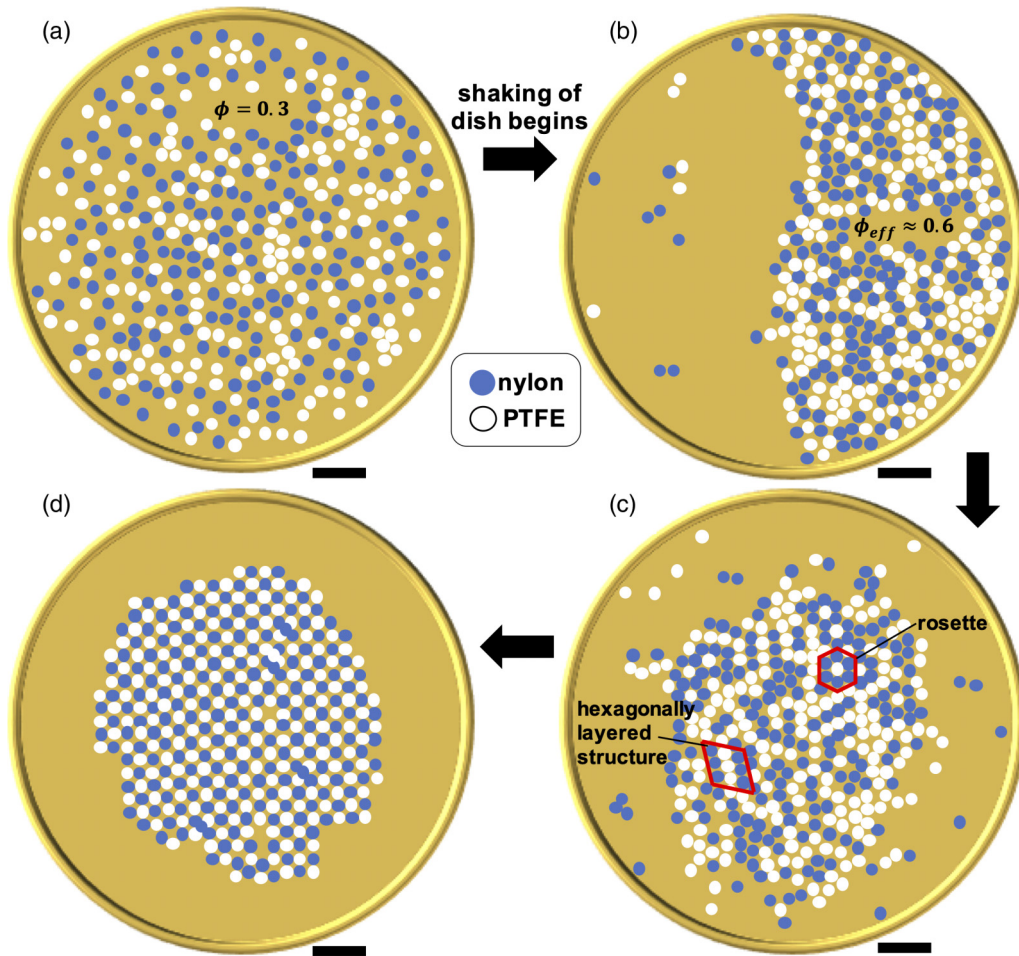†gwhitesides@gmwgroup.harvard.edu

FIG. 1. Schematic of the formation of an electrostatically self-assembled material. (a) The dish contains 400 beads, which cover approximately 30% of the surface area of the dish. (b) As the dish is shaken, the beads undergo inelastic collisions, and their velocities are correlated. Their effective density is nearly double the fractional surface area coverage of beads on the dish. (c) The beads form hexagonally coordinated transient structures that we call *rosettes* and, in certain instances, hexagonally layered structures. (d) Finally, the beads undergo further rearrangements to form an energy-minimized structure. Here, for the case of equal numbers of nylon and polytetrafluoroethylene (PTFE) beads, the final structure has square symmetry. All scale bars correspond to 10 mm (about 4.2 bead diameters).

tribocharge. Tribocharging is the process by which a material becomes charged upon contact with another material [9–11]. Nylon charges positively, while PTFE charges negatively [9]. We find that the magnitude of the charge, which is on the order of hundreds of picocoulombs per bead, depends on the relative number of nylon and PTFE beads present in the dish. Shaking experiments are performed at a controlled humidity of ≈20% RH. Some theories relate the tribocharging of two nonionic polymers to the redistribution of hydroxide ions, during contact, in their surface layers of absorbed water [9,12–14]. Thus, control of the relative humidity is important for reproducible results.

II. MATERIALS AND METHODS

As depicted in Fig. S8 in the Supplemental Material [8], the entire shaking apparatus is enclosed in a humidity-controlled chamber. Our experiments are conducted at ≈20% RH. We adjust the humidity by injecting wet and/or dry nitrogen into the chamber. Over the course of 2 h, we monitor the humidity in the chamber using a hygrometer probe (VWR Traceable

Thermometer/Hygrometer) and adjust nitrogen levels accordingly. After 2 h, we begin the experiment. The beads are initially uncharged; we discharge the beads with a Zerostat antistatic gun (VWR). The dynamics are recorded using a high-speed color video camera (Phantom v310) with a wide-angle lens attachment (Tokina 12–24 mm f4) at a resolution of 640×480 pixels and a frame rate of 600 frames per second. The lens is enclosed in the chamber, while the body of the camera is outside the chamber. The camera is mounted overhead.

In each experiment, we use a combined total of 400 beads that are reported by the manufacturer to be 2.38125 mm in diameter. The beads are made from nylon 6,6 (McMaster Carr 9613K12) and PTFE (McMaster Carr 9660K12). The nylon beads are dyed blue by adding ≈20 mg of Disperse Blue 14 (Sigma Aldrich) to 100 nylon beads, 2 mL of isopropyl alcohol, and 8 mL of Milli-Q water; the mixture is heated at 60 °C overnight with continuous stirring. The beads are rinsed with isopropyl alcohol and, subsequently, with 200 proof ethyl alcohol until the supernatant is clear. PTFE beads are not dyed, but they too are rinsed with 200 proof ethyl alcohol

before use. All beads are oven dried at 40–60 °C. In certain control experiments, we use nylon beads coated with gold; beneath the gold layer, there is an adhesive layer of chromium.

The appropriate number of nylon and PTFE beads is placed in a gold-coated, polystyrene Petri dish (Corning) with an inner diameter of approximately 86.3 mm. The interior of the dish is coated with, in sequence, an adhesive layer of chromium ($\approx 5-15$ nm in thickness) and a continuous gold film (≈ 300 nm in thickness). Our choice of gold is motivated by the fact that it sits roughly halfway between nylon and PTFE on the triboelectric series [5,6,9]. The Petri dish is ungrounded and sits on the platform of an orbital or linear shaker. The orbital shaker (VWR Orbital Shaker Standard 1000) has an orbital diameter of 15 mm and a speed range of 40–300 rpm. The linear shaker (VWR Reciprocating Shaker Advanced 3750) has a stroke length of 19 mm and a speed range of 20–300 strokes per minute (spm). Unless otherwise noted, all experiments are conducted at 300 rpm or 300 spm. The platform of the shaker is covered with a thin film of PTFE to reduce the coefficient of friction between the dish and the platform. The Petri dish is confined to a portion of the platform area by a solid 3D-printed enclosure made from acrylonitrile butadiene styrene plastic. As the shaker moves, the dish knocks into the boundaries of the enclosure at random. On the rim of the dish, we affix three equally spaced black beads (1.5875 mm in diameter) to white double-sided mounting tape. We determine the center coordinates of the dish in time by tracking the three beads and fitting a circle to their positions.

We locate the beads in each frame and classify them as nylon or PTFE using our custom-built, Python-based software package. Our package combines Hue Saturation Value (HSV) image thresholding, image sharpening, and watershed segmentation [15] to identify the center of each bead. We recover the positions of the beads in the frame of reference of the moving dish by subtracting the coordinates of the center of the dish from the coordinates of each bead. To analyze the kinetics of formation, we determine the Voronoi tessellation [16] for the arrangement of beads in each frame, and we calculate the local bond-order parameter for each bead within the arrangement [17]. We report the former values for frames where at least 90% of the beads are identified by our algorithm, and the latter values for frames where at least 90% of each type of bead are identified. The Voronoi tessellation is composed of cells—with one bead associated with each cell. The cell corresponds to the locus of points that are closer to the bead in question than to any other bead [16]. We calculate the area of each cell; the local area density is the cross-sectional area of the bead divided by the area of its Voronoi cell. We exclude any cells from our analysis whose vertices do not lie within the confines of the dish and whose corresponding local area fraction is greater than one. The latter case arises when beads are falsely detected, which sometimes results in the seeming appearance of overlapping beads that together occupy an area greater than the Voronoi cell. The local bond-order parameter for a bead, denoted by l, in an assembly is

$$\psi_k(l) = \frac{1}{n} \sum_{j=1}^{n} \exp(ik\phi_{lj}),$$

where we sum over the n beads closest to bead l, and ϕ_{lj} is the angle between the vector $\vec{r}_{lj}$, drawn from bead l to bead j, and the positive x axis [18]. We set $n = k$ such that we consider the k neighbors closest to a bead of interest. To determine the trajectory of select particles, we resort to a Python [19] implementation of the Crocker-Grier algorithm [20]. From the trajectory, we can determine the mean-squared displacement of the bead relative to its initially tracked position.

To measure the charge of each individual bead, we designed what we call a Faraday tube apparatus [11,21], as depicted schematically in Fig. S9 in the Supplemental Material [8]. The apparatus, which spans ≈ 2 m in height, consists of two nested aluminum tubes that are encased by insulators and electrically connected via the Zurich Instruments MFIA Impedance Analyzer. The innermost tube is made of polypropylene; its top extremity is connected to house vacuum. When a bead is placed in the bottom end of the polypropylene tube, it is drawn through the length of the apparatus by the vacuum. The outer aluminum tube is actively maintained at 0 V by the Impedance Analyzer, while the inner aluminum tube is connected to ground. When a charged bead enters the apparatus, by induction, charges flow to/from ground until the charge residing on the inner surface of the inner aluminum tube is equal in magnitude to the charge of the bead. This condition ensures that there is no electrical flux through the conductor, namely, the inner aluminum tube.

The Impedance Analyzer records the current traveling into/from the inner aluminum tube over time. When a positively (negatively) charged bead enters the tube, the current reading goes from zero to a local maximum (minimum) and back to zero; according to conventional current nomenclature, this means that positive charge carriers move from (to) the inner aluminum tube. No current flows to the inner aluminum tube as the bead traverses the tube. When the bead exits the tube, the current flows in the opposite direction to restore zero charge on the inner surface of the inner aluminum tube. This process is depicted in Fig. S10 in the Supplemental Material [8]. The charge on the bead corresponds to the time integral of the first current peak (negative or positive). Since the flow of air in the polypropylene tube is turbulent, we only consider the signal as the bead enters the tube because it may undergo further collisions during its traversal of the apparatus. It is worth noting, however, that there is a segment of polypropylene tubing that extends beyond the aluminum tubes so that the entry port for the beads is situated at table height. Each bead is removed from the dish with polybutylene terephthalate tweezers (Rubis K7), which have been shown to minimize charge dissipation [22], and placed inside the entry port. Before making the measurements, the dish is moved from the humidity-controlled chamber to the table beside the Faraday tube apparatus; every effort is made by the experimenter to keep the dish straight to prevent discharge events.

III. RESULTS

A. Two-stage formation of Coulombic materials

The formation of our Coulombic materials occurs in two stages: (i) the formation of transient structures and (ii) the
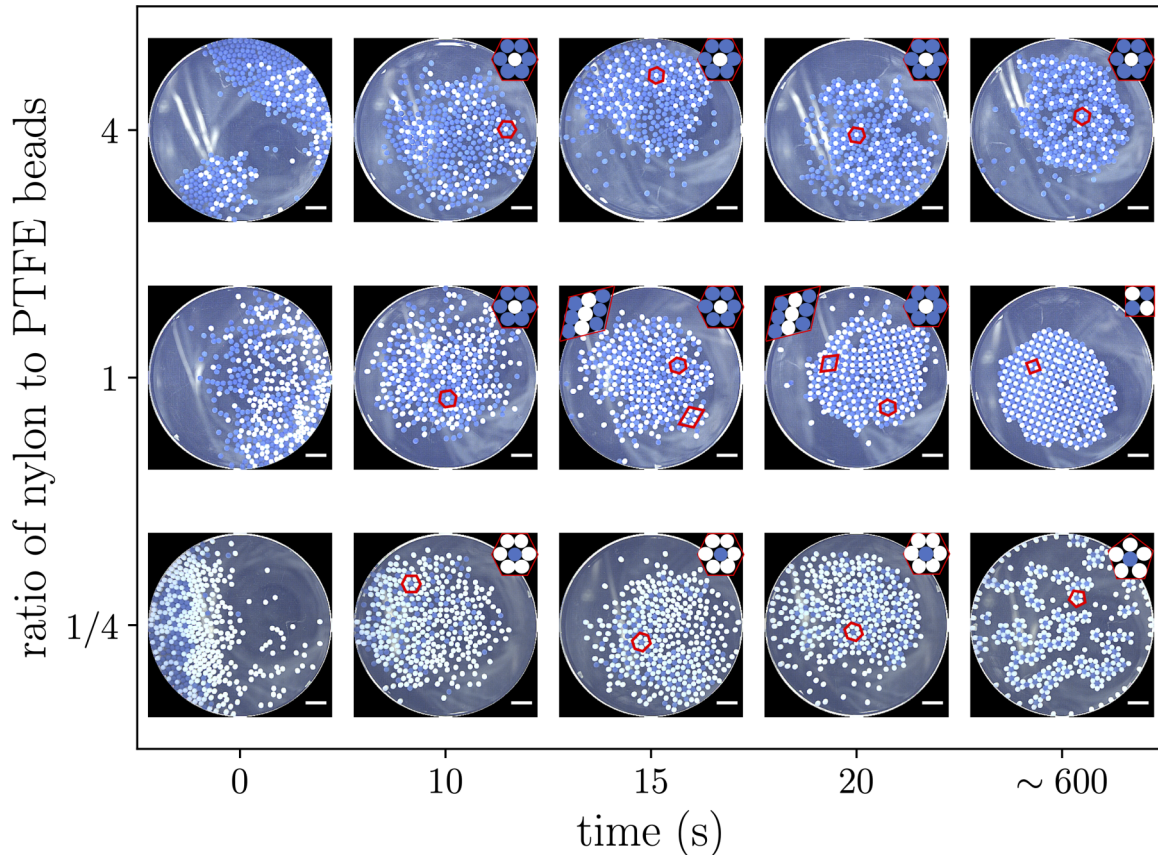
FIG. 2. Snapshots of the formation of the material in time for the cases of $N_{\text{nylon}}/N_{\text{PTFE}} = \{\frac{1}{4}, 1, 4\}$. Important structures are outlined in red and reproduced in expanded form in the insets. In each experiment, 400 beads are agitated with an orbital shaker. The color of the images is adjusted for improved contrast. All scale bars correspond to 10 mm (about 4.2 bead diameters).

formation of final structures. The formation of transient structures is influenced by the method of agitation and the tribocharging of the beads. As the beads are agitated with an orbital or a linear shaker, they undergo inelastic collisions with the dish and with each other. Their velocities are also correlated. As a result, the beads move as an ensemble, and, at any moment in time, they are not randomly distributed on the surface of the dish. Their effective local density is close to $\phi_{\text{eff}} \approx 0.6$, as reflected schematically in Fig. 1(b) and as measured in Fig. S4 in the Supplemental Material [8]. This effective density is nearly twice the fraction of the area of the dish that the beads occupy, $\phi = 0.3$, and it corresponds to the average of all local area densities. A local area density is the cross-sectional area of the bead divided by the area of its respective Voronoi cell [16] (details in Materials and Methods). During this early stage of material formation, it follows that the beads are close-packed and that rosettes—locally ordered, close-packed structures—commonly occur. A rosette is a structure in which a central bead is surrounded by six beads of the opposite kind, as outlined in Fig. 1(c). We hypothesize that rosettes arise as a means of screening the charge of the central bead, which is the more heavily charged of the two species in the rosette. Next, as the beads continue to tribocharge, they transition to a final structure that minimizes the total Coulombic energy of the system. As illustrated in Fig. 1(d), for the case of $N_{\text{nylon}}/N_{\text{PTFE}} = 1$, the beads rearrange into a square lattice.

The formation of Coulombic materials also occurs in two stages for the cases of $N_{\text{nylon}}/N_{\text{PTFE}} = \{\frac{1}{4}, 4\}$. In Fig. 2, we reproduce findings from three experiments performed on an orbital shaker in which the relative number of nylon and PTFE beads is altered, while maintaining the total number of beads at 400. Clearly, the final structures—recovered after concluding approximately 10 min (or 600 s) of shaking—are very different, although the transient structures are strikingly similar. For the case of $N_{\text{nylon}}/N_{\text{PTFE}} = 1$, as highlighted in the second row of Fig. 2, hexagonally layered structures occur in addition to the occasional appearance of PTFE-centered rosettes. We define *hexagonally layered structures* as alternating rows of nylon and PTFE beads that are stacked in 2D to minimize void space. For the case of $N_{\text{nylon}}/N_{\text{PTFE}} = \frac{1}{4}$, nylon-centered rosettes are common transient structures. Eventually, they give way to a final, open structure composed of *pentagonal rosettes*, which are repeating units in which a central nylon bead is surrounded by five PTFE beads. It is geometrically prohibited for a close-packed structure of pentagonal rosettes to occur when all beads are equal in size [23]. For the case of $N_{\text{nylon}}/N_{\text{PTFE}} = 4$, PTFE-centered rosettes appear as both transient and final structures, as shown in the third row of Fig. 2. Similar structure transitions occur when the same experiments are carried out on a linear shaker (Fig. S5 in the Supplemental Material [8]). For $N_{\text{nylon}}/N_{\text{PTFE}} = 1$, however, the case of the linear shaker differs from that of the orbital shaker insofar as portions of the final structure oscillate between a square
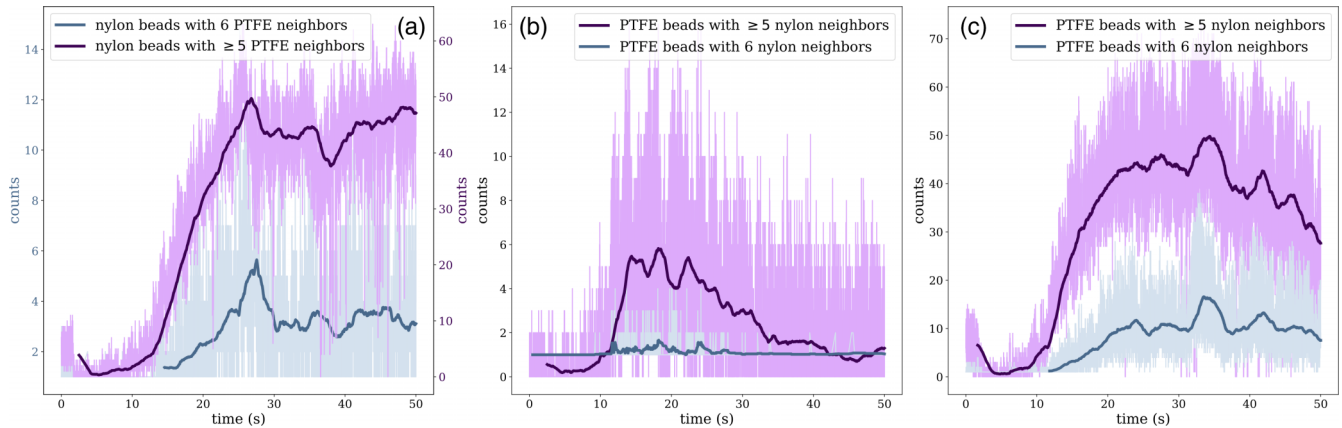
FIG. 3. Number of beads with at least five nearest neighbors of the opposite kind and number of rosettes for the cases of (a) $N_{\mathrm{nylon}}/N_{\mathrm{PTFE}} = \frac{1}{4}$, (b) $N_{\mathrm{nylon}}/N_{\mathrm{PTFE}} = 1$, and (c) $N_{\mathrm{nylon}}/N_{\mathrm{PTFE}} = 4$. A polytetrafluoroethylene (PTFE)- or nylon-centered rosette is a structure in which a PTFE or nylon bead is surrounded by six nylon or PTFE nearest neighbors, respectively. A surrounding bead must be located within 1.2 bead diameters of the central bead to be counted as a nearest neighbor. In each experiment, 400 beads are agitated with an orbital shaker. Each bolded trendline represents a rolling average of the raw data, which in turn is depicted in the corresponding lightened hue.

lattice and a hexagonally layered structure due to periodic shear transformations of the crystal due to the motion of the shaker.

B. First stage: Formation of transient structures

Clearly, transient rosette structures are common to all cases of $N_{\mathrm{nylon}}/N_{\mathrm{PTFE}}$. To understand why they occur, we consider two factors that are linked to their appearance: (i) mechanical agitation and (ii) the tribocharging of beads. First, we isolate the mechanics of shaking from tribocharging by conducting a set of control experiments in which we agitate 400 gold-coated nylon beads, each measuring about 2.38 mm in diameter, in the gold-coated Petri dish. Gold-coated nylon beads do not tribocharge appreciably on a gold surface (Fig. S1 in the Supplemental Material [8]). The velocities of randomly selected gold-coated beads are highly correlated (Figs. S2 and S3 in the Supplemental Material [8]). When we plot for a sequence of frames the coordinates of each gold-coated bead with the center of mass of the ensemble of beads subtracted from the respective coordinates of each bead and play through such frames, then we observe local density waves traveling through the ensemble of beads in time as they collide with the walls of the dish. Thus, the method of shaking drives the beads into early-stage, closed-packed structures as confirmed by mean local packing fractions (or densities) ranging from 0.5 to 0.6 (Fig. S4 in the Supplemental Material [8]). Second, we consider the local order in the transient structures as it relates to tribocharging. In Fig. 3, we plot the number of rosettes and the number of beads with at least five nearest neighbors of the opposite kind. Regardless of the relative number of nylon and PTFE beads, the number of rosettes increases after about 10 s of agitation. While the increase in PTFE-centered rosettes is negligible for the case of $N_{\mathrm{nylon}}/N_{\mathrm{PTFE}} = 1$, as per the blue trendline in Fig. 3(b), we observe a strong increase in the number of PTFE beads with at least five nylon neighbors near the 10-s mark. Rosettes are most prevalent in the case of $N_{\mathrm{nylon}}/N_{\mathrm{PTFE}} = 4$, since the final structure is composed of repeating PTFE-centered rosettes. The formation of these

transient rosettes is indeed related to tribocharging. As per Fig. S7 in the Supplemental Material [8], around the 10-s mark, the magnitude of the charge of the type of bead that sits at the center of a rosette is on average greater than that of the type that surrounds the central bead in a rosette. Thus, the six beads surrounding the central bead of a rosette serve as charge screening barriers to minimize the repulsions between central beads. In fact, the appearance of nylon- or PTFE-centered rosettes coincides with a local maximum in the average bond length between every nylon or PTFE bead and its nearest six nylon or PTFE neighbors, respectively, as shown in Fig. S6 in the Supplemental Material [8]. This finding indicates that rosettes maximize the distance between central beads when the beads are close-packed.

C. Second stage: Formation of final structures

The transition between the transient and final structures can be monitored by considering the average of the moduli of the local k-atic bond order parameters for all the beads, $\langle|\psi_k|\rangle$, in time. The k-atic bond order parameter, ψ_k, provides a measure of the k-order symmetry of a bead within the crystal; it is complex-value, and its magnitude, $|\psi_k|$, ranges from zero to one. $|\psi_k| = 1$ corresponds to a bead with perfect k-order symmetry (see Materials and Methods for more details). For each case of $N_{\mathrm{nylon}}/N_{\mathrm{PTFE}}$, we consider the evolution of $\langle|\psi_k|\rangle$ for the beads of the type that sit at the center of the transient rosettes relative to their neighbors of the opposite type. For example, in the case of $N_{\mathrm{nylon}}/N_{\mathrm{PTFE}} = \frac{1}{4}$, we consider $\langle|\psi_k|\rangle$ for all nylon beads relative to their PTFE neighbors. Initially, for all three relative ratios of nylon and PTFE beads, $\langle|\psi_3|\rangle$ is the largest of the order parameters. For the case of $N_{\mathrm{nylon}}/N_{\mathrm{PTFE}} = 1$, the local maximum in $\langle|\psi_3|\rangle$ at approximately the 15-s mark stems from the fact that, in a close-packed structure containing equal numbers of nylon and PTFE beads, on average, half of the six nearest neighbors of any bead will be of a different kind. Eventually, $\langle|\psi_4|\rangle$ overtakes $\langle|\psi_3|\rangle$, which reflects the fourfold symmetry of the final structure. In the inset of Fig. 4(b), we sketch some
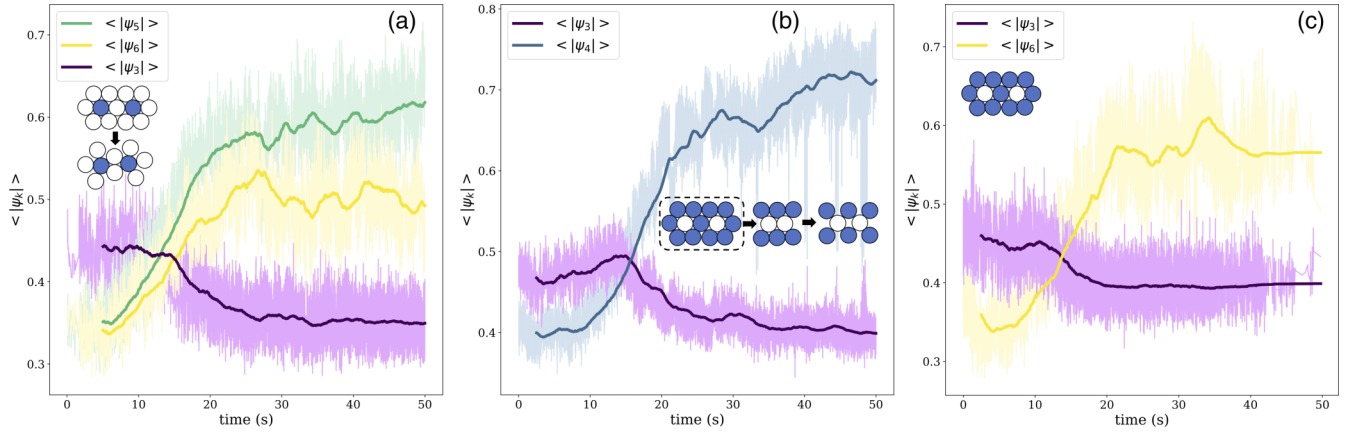
FIG. 4. Average of the modulus of the *k*-atic local bond order parameter, where $k = \{3, 4, 5, 6\}$, for (a) all nylon beads in relation to their polytetrafluoroethylene (PTFE) neighbors when $N_{\text{nylon}}/N_{\text{PTFE}} = \frac{1}{4}$ and all PTFE beads in relation to their nylon neighbors when (b) $N_{\text{nylon}}/N_{\text{PTFE}} = 1$ and (c) $N_{\text{nylon}}/N_{\text{PTFE}} = 4$. Frames are only included in the analysis if at least 90% of the beads of each type are detected. Each bolded trendline represents a rolling average of the raw data, which in turn is depicted in the corresponding lightened hue. In each experiment, 400 beads are agitated with an orbital shaker. (insets) Common transient and final structures are illustrated schematically in the insets of (a)–(c).

of the local rearrangements that we observe between beads that result in a square lattice. PTFE-centered rosettes, however seldom they occur, transition to a hexagonally layered structure by 'expelling' two nylon beads. By shear transformation, a hexagonally layered structure transitions to a square lattice. For the case of $N_{\text{nylon}}/N_{\text{PTFE}} = 4$, the time at which $\langle |\psi_6| \rangle$ surpasses $\langle |\psi_3| \rangle$ coincides with the appearance of PTFE-centered rosettes. Eventually, $\langle |\psi_6| \rangle$ becomes the largest order parameter as the PTFE-centered rosettes persist in time. For the case of $N_{\text{nylon}}/N_{\text{PTFE}} = \frac{1}{4}$, $\langle |\psi_5| \rangle$ becomes the largest order parameter, as the final structure is composed of pentagonal rosettes. We suspect that transient, nylon-centered rosettes shed a PTFE neighbor to minimize local repulsions between neighboring PTFE beads. This loss of a neighboring bead may not occur for the case of $N_{\text{nylon}}/N_{\text{PTFE}} = 4$ because, after 10 min of agitation, the average magnitude of the charge of the nylon beads is less than that of PTFE beads for the case of $N_{\text{nylon}}/N_{\text{PTFE}} = \frac{1}{4}$, as per Fig. S7 in the Supplemental Material [8]. Regardless of the relative ratio of nylon and PTFE beads, the symmetry of the structure after about 50 s of shaking remains largely unchanged relative to the final structure, obtained after a total of about 600 s of shaking. As the shaking continues, further rearrangements occur such that a more defect-free final structure emerges.

As we have shown, the symmetries of the final structures may be different than those of their transient structures. Ultimately, the beads continue to undergo rearrangements until they achieve structures that minimize the total Coulombic energy of the system. The total Coulombic energy refers to the sum of all pairwise Coulombic energies, without duplication, between beads and their image charges [7]. We approximate the beads as point charges and assume that the image charges, also modeled as point charges, sit below their centers on the surface of the ungrounded gold-coated Petri dish. To calculate the Coulombic energy in time, we conduct a series of experiments whereby we shake the beads for a given amount of time, take a picture of the arrangement of beads after the shaking has ended, and measure the charge of all the beads while keeping track of their positions on the dish (within the

cluster, at its edge, or along the perimeter of the dish). To measure the charge on an individual bead, we run it through a homemade charge-measuring apparatus, fashioned on the work of our colleagues [11] and inspired by the Faraday pail [21] (details in Materials and Methods). We assign at random a charge to each bead from the empirically established charge distribution of nylon or PTFE beads and calculate its positional information from the captured image. The image charge is assigned a charge equal in magnitude but opposite in sign to the bead directly above it. We calculate the Coulombic energy for the system, reiterate this process 200 times, and report the resultant distribution of energies (Fig. 5). We note a steady decrease in the Coulombic energies of the system over time for all three cases of $N_{\text{nylon}}/N_{\text{PTFE}}$. The final value of the Coulombic energy of the system depends on $N_{\text{nylon}}/N_{\text{PTFE}}$: nylon and PTFE tribocharge up to different values (Fig. S7 in the Supplemental Material [8]) depending on the frequency of collisions that they undergo with beads of the same kind.

Local bead rearrangements drive the transition from transient to final structures. Rearrangements are enabled by vigorous mechanical agitation. The beads move about the dish, undergo collisions, tribocharge, and rearrange themselves. Over time, beads are attracted to beads of the opposite charge and form aggregates. The beads also interact electrostatically with the gold-coated substrate. If the shaking is too weak, the beads will not have enough kinetic energy to rearrange within the aggregates. To confirm this hypothesis, we conduct a set of experiments where we consider the final structures that form upon shaking 200 nylon beads and 200 PTFE beads on an orbital shaker for 10 min at three centripetal accelerations: 1.85 m/s^2, 3.6 m/s^2, and 7.4 m/s^2. The centripetal acceleration of 7.4 m/s^2 corresponds to that at which we normally perform all experiments. At centripetal accelerations of 1.85 m/s^2 and 3.6 m/s^2, the beads do not have sufficient kinetic energy to undergo rearrangements with their nearest neighbors. This lack of energy results in disordered aggregates or crystals containing defects (Fig. 6). Given the limited extent of rearrangements in the structures, the beads do not tribocharge as appreciably as they do at an acceleration of
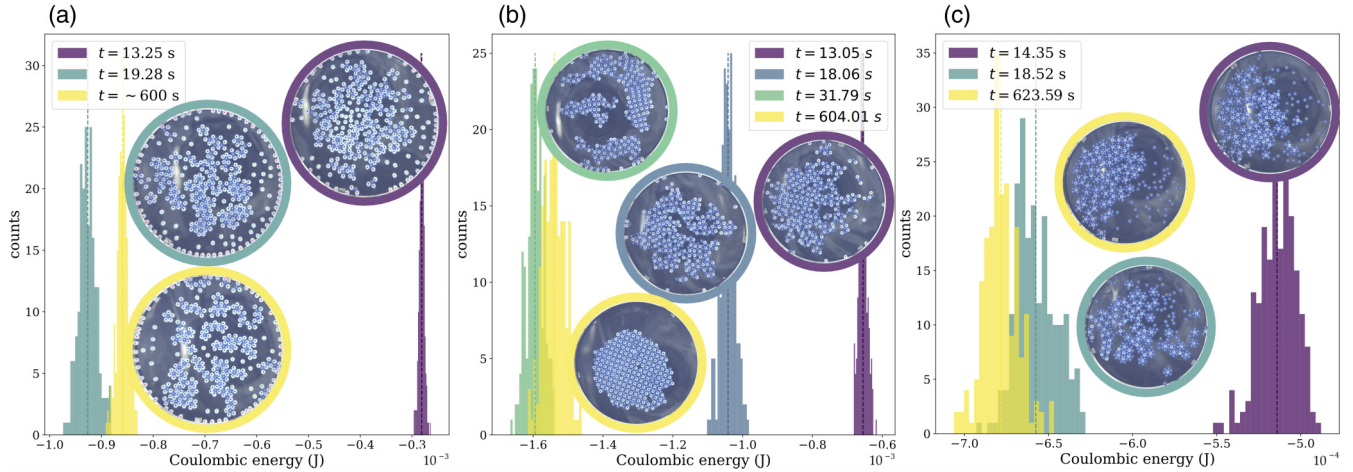
FIG. 5. The evolution in time of the Coulombic energy of the system when accounting for image charges on the surface of the gold-coated dish for the cases of (a) $N_{nylon}/N_{PTFE} = \frac{1}{4}$, (b) $N_{nylon}/N_{PTFE} = 1$, and (c) $N_{nylon}/N_{PTFE} = 4$. The structures at each point in time are shown in the insets. The beads that are included in the calculation are marked by dots in white or yellow (nylon) and black, green, or red [polytetrafluoroethylene (PTFE)] depending on their positions in the dish. The energy is reported as a distribution because the calculation is repeated 200 times.

7.4 m/s^2, which manifests in lower magnitudes of Coulombic binding energies.

IV. DISCUSSION

Our results show that the final material structures are stable in time, reproducible, and largely indifferent to the kind of agitation (orbital or linear). Several real-world examples in different material systems, including mechanical alloying [24] or ion beam mixing [25], provide evidence that suggests that out-of-equilibrium processes such as ours can in fact yield equilibrium structures. The characterization of the final structures could enable the design of binary Coulombic materials. Shaking could even be suspended at intermediate stages to produce materials from transient structures. In fact,

our complete understanding of the transient phases in the formation of Coulombic materials tells us that the symmetry of the final structures could be altogether different from that of the transient phases. The symmetry of the final structure that we observe is dictated by the relative number of nylon and PTFE beads. The kinetics of formation of the structures largely depends on the frequency and magnitude of agitation and the rate of tribocharging of the beads. Rosettes tend to be the transient structures regardless of the final structures.

We conclude that three processes influence the formation of Coulombic materials. First, the method of agitation influences the early-stage close-packing of the beads. The agitation of the beads in this system is akin to stirring. The beads move as an ensemble, their velocities are correlated, and they undergo inelastic collisions. They do not independently explore

$$\langle E_{Coulombic} \rangle = -0.51 \times 10^{-3} \text{ J} \quad \langle E_{Coulombic} \rangle = -1.20 \times 10^{-3} \text{ J} \quad \langle E_{Coulombic} \rangle = -1.54 \times 10^{-3} \text{ J}$$
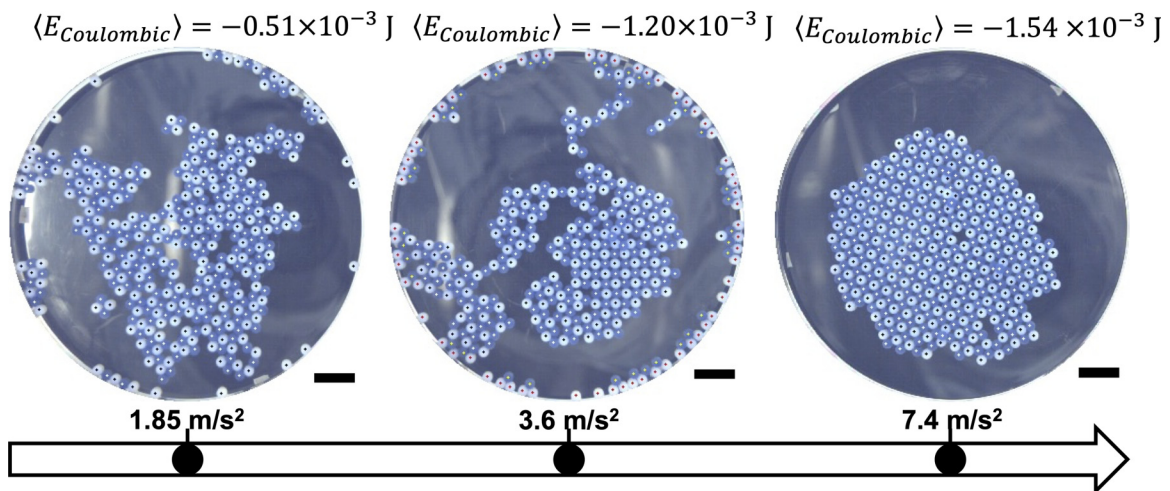

FIG. 6. Mechanical shaking helps in the formation of a final ordered structure. (from left to right) By increasing the centripetal acceleration of an orbital shaker from 1.85 m/s^2 to 7.4 m/s^2, a mixture of 200 nylon beads and 200 polytetrafluoroethylene (PTFE) beads adopts an increasingly ordered final structure after 10 minutes of shaking. The total Coulombic energy of the system, accounting for image charges, at each centripetal acceleration is reported. The beads that are included in the calculation are marked by dots in white or yellow (nylon) and black or red (PTFE) depending on their positions in the dish. All scale bars correspond to 10 mm (about 4.2 bead diameters).

the surface of the dish. Instead, the beads are close-packed, and their effective local area density, as calculated from the fraction of the area of each Voronoi cell that is occupied by a bead, is nearly twice the value of the fractional area coverage of the beads on the dish. Second, the tribocharging of beads influences the local order of transient structures. The magnitude of tribocharging of the beads depends on the relative number of nylon and PTFE beads. Tribocharging plays a role in defining the local order of transient structures. We note the common occurrence of rosettes for all cases of $N_{\mathrm{nylon}}/N_{\mathrm{PTFE}}$, although for the case of $N_{\mathrm{nylon}}/N_{\mathrm{PTFE}} = 1$, they appear less frequently than hexagonally layered structures. The appearance of rosettes coincides with a local maximum in the distance between the highly charged, central beads of the structures. This evidence suggests that rosette structures are a preferable arrangement for charge shielding. Third, the minimization of the Coulombic energy of the system, namely, the dish and the beads, drives late-stage bead rearrangements. As the beads continue to tribocharge, they will continue to rearrange such that they ultimately adopt a structure that minimizes the total Coulombic energy of the system. Mechanical shaking is the key to imparting sufficient kinetic energy to each bead to enable such local rearrangements. The symme-

try of the final structure is not necessarily the same as that of the transient one. Our characterization of the kinetics of formation of binary Coulombic materials composed of nylon and PTFE opens the door to new possibilities for materials synthesis, provides insights into solid-solid phase transitions, and challenges common conceptions about the symmetry of seedlike structures in nucleation.

[1] T. Nakamuro, M. Sakakibara, H. Nada, K. Horano, and E. Nakamura, Capturing the moment of emergence of crystal nucleus from disorder, J. Am. Chem. Soc. **143**, 1763 (2021).

[2] M. E. Leunissen, C. G. Christova, A.-P. Hynninen, C. P. Royall, A. I. Campbell, A. Imhof, M. Dijkstra, R. van Roij, and A. van Blaaderen, Ionic colloidal crystals of oppositely charged particles, Nature (London) **437**, 235 (2005).

[3] T. Hueckel, G. M. Hocky, J. Palacci, and S. Sacanna, Ionic solids from common colloids, Nature (London) **580**, 487 (2020).

[4] A. M. Kalsin, M. Fialkowski, M. Paszewski, S. K. Smoukov, K. J. Bishop, and B. A. Grzybowski, Electrostatic self-assembly of binary nanoparticle crystals with a diamond-like lattice, Science **312**, 420 (2006).

[5] B. A. Grzybowski, A. Winkleman, J. A. Wiles, Y. Brumer, and G. M. Whitesides, Electrostatic self-assembly of macroscopic crystals using contact electrification, Nat. Mater. **2**, 241 (2003).

[6] R. Cademartiri, C. A. Stan, V. M. Tran, E. Wu, L. Friar, D. Vulis, L. W. Clark, S. Tricard, and G. M. Whitesides, A simple two-dimensional model system to study electrostatic-self-assembly, Soft Matter **8**, 9771 (2012).

[7] J. D. Jackson, *Classical Electrodynamics*, 3rd ed. (Wiley, New York, 1999).

[8] See Supplemental Material at http://link.aps.org/supplemental/10.1103/PhysRevMaterials.7.L040401 for the additional reference material.

[9] L. McCarty and G. M. Whitesides, Electrostatic charging due to separation of ions at interfaces: Contact electrification of ionic electrets, Angew. Chem. Int. Ed. **47**, 2188 (2008).

[10] W. R. Harper, *Contact and Frictional Electrification* (Laplacian Press, Morgan Hill, California, 1998).

[11] L. S. McCarty, A. Winkleman, and G. M. Whitesides, Ionic electrets: Electrostatic charging of surfaces by transferring mobile ions upon contact, J. Am. Chem. Soc. **129**, 4075 (2007).

[12] A. Schella, S. Herminghaus, and M. Schröter, Influence of humidity on tribo-electric charging and segregation in shaken granular media, Soft Matter **13**, 394 (2017).

[13] D. J. Lacks and T. Shinbrot, Long-standing and unresolved issues in triboelectric charging, Nat. Rev. Chem. **3**, 465 (2019).

[14] I. A. Harris, M. X. Lim, and H. M. Jaeger, Temperature dependence of nylon and PTFE triboelectrification, Phys. Rev. Mater. **3**, 085603 (2019).

[15] S. Beucher and F. Meyer, The morphological approach to segmentation: The watershed transformation, in *Mathematical Morphology in Image Processing*, edited by E. R. Dougherty (CRC Press, Boca Raton, 1993), pp. 433–481.

[16] E. A. Lazar and A. Shoan, Voronoi chains, blocks, and clusters in perturbed square lattices, J. Stat. Mech. (2020) 103204.

[17] V. Ramasubramani, B. D. Dice, E. S. Harper, M. P. Spellings, J. A. Anderson, and S. C. Glotzer, Freud: A software suite for high throughput analysis of particle simulation data, Comput. Phys. Commun. **254**, 107275 (2020).

[18] D. R. Nelson, M. Rubinstein, and F. Spaepen, Order in two-dimensional binary random arrays, Philos. Mag. A **46**, 105 (1982).

[19] D. B. Allan, T. Caswell, N. C. Keim, C. M. van der Wel, and R. W. Verweij, Soft-matter/trackpy: Trackpy v0.5.0 (v0.5.0), Zenodo (2021).

[20] J. C. Crocker and D. G. Grier, Methods of digital video microscopy for colloidal studies, J. Colloid Interface Sci. **179**, 293 (1996).

[21] M. Faraday, XXXII. On static electrical inductive action, Lond. Edinb. Dublin. Philos. Mag. J. Sci. **22**, 200 (1843).

[22] S. Siowling, S. W. Kwok, H. Liu, and G. M. Whitesides, Contact de-electrification of electrostatically charged polymers, J. Am. Chem. Soc. **134**, 20151 (2012).

[23] H. Hiller, The crystallographic restriction in higher dimensions, Acta Cryst. **A41**, 541 (1985).

[24] C. Suryanarayana, Mechanical alloying and milling, Prog. Mater. Sci. **46**, 1 (2001).

[25] R. S. Averback, Fundamental aspect of ion beam mixing, Nucl. Instrum. Meth. Phys. Res. B **15**, 675 (1986).